Computers & Geosciences 60 (2013) 11–22

Contents lists available at SciVerse ScienceDirect

Computers & Geosciences

journal homepage: www.elsevier.com/locate/cageo

Fracture network evaluation program (FraNEP): A software for analyzing 2D fracture trace-line maps

Conny Zeeb [a,b,d,*], Enrique Gomez-Rivas [b], Paul D. Bons [b], Simon Virgo [c], Philipp Blum [a]

[a] Karlsruhe Institute of Technology (KIT), Institute for Applied Geosciences (AGW), Kaiserstraße 12, 76131 Karlsruhe, Germany
[b] University of Tübingen, Department of Geosciences, Wilhelmstraße 56, 72074 Tübingen, Germany
[c] RWTH Aachen University, Structural Geology Tectonics Geomechanics, Lochnerstrasse 4-20, 52056 Aachen, Germany
[d] Geotechnical Institute, TU Bergakademie Freiberg, Gustav-Zeuner-Str. 1, 09596 Freiberg, Germany

ARTICLE INFO

Article history:
Received 25 June 2012
Received in revised form
6 February 2013
Accepted 17 April 2013
Available online 31 May 2013

Keywords:
Fracture network analysis
Fracture sampling
Sampling methods
Fracture density

ABSTRACT

Fractures, such as joints, faults and veins, strongly influence the transport of fluids through rocks by either enhancing or inhibiting flow. Techniques used for the automatic detection of lineaments from satellite images and aerial photographs, LIDAR technologies and borehole televiewers significantly enhanced data acquisition. The analysis of such data is often performed manually or with different analysis software. Here we present a novel program for the analysis of 2D fracture networks called FraNEP (Fracture Network Evaluation Program). The program was developed using Visual Basic for Applications in Microsoft Excel™ and combines features from different existing software and characterization techniques. The main novelty of FraNEP is the possibility to analyse trace-line maps of fracture networks applying the (1) scanline sampling, (2) window sampling or (3) circular scanline and window method, without the need of switching programs. Additionally, binning problems are avoided by using cumulative distributions, rather than probability density functions. FraNEP is a time-efficient tool for the characterisation of fracture network parameters, such as density, intensity and mean length. Furthermore, fracture strikes can be visualized using rose diagrams and a fitting routine evaluates the distribution of fracture lengths. As an example of its application, we use FraNEP to analyse a case study of lineament data from a satellite image of the Oman Mountains.

1. Introduction

Mechanical discontinuities have a significant influence on the transport of fluids in the subsurface, for example in fractured oil and gas reservoirs or aquifers. Since the terminology for mechanical defects in rocks is diverse and often has genetic connotations, we will refer to the term “fractures” to include linear structures such as fractures, joints or veins. Fluid flow and transport through a fractured medium can be simulated by discrete fracture network (DFN) modelling (e.g. Blum et al., 2009). The DFN concept is commonly used to translate deterministic and/or statistical information on the geometry of fracture networks into equivalent fluid flow properties (i.e. permeability, hydraulic conductivity or hydraulic fracture aperture) along them. A detailed review of these concepts as well as the characterization of flow and transport behaviour in fractured media is provided, for example, by Neuman (2005).

In DFN models each fracture is individually represented with all its geometric parameters (i.e. fracture length and aperture). Typical geometric parameters used to describe fracture networks are fracture density, intensity, orientation, mean length or length distribution (Priest, 1993). The hydraulic properties influencing the fluid transport through a DFN include mechanical or hydraulic fracture aperture, displacement along fractures, mineral precipitates on fracture walls and mechanical properties of the host rock (Lee and Farmer, 1993). The most widely used methods to acquire these geometric parameters from outcrops or well cores are: (1) scanline sampling (e.g. Priest and Hudson, 1981), (2) window sampling (e.g. Pahl, 1981), and (3) circular scanline and window sampling (e.g. Mauldon et al., 2001). From now we will refer to the latter as the circular estimator method.

DFN models are typically treated in a stochastic framework (Berkowitz, 2002). Based on the aforementioned parameters, multiple realizations of fracture networks are often studied using Monte Carlo analysis (e.g. Blum et al., 2005; 2009). Several open access and commercial programs are available for the generation of artificial DFNs and subsequent analysis of their fluid flow

* Corresponding author at: TU Bergakademie Freiberg, Geotechnical Institut, Gustav-Zeuner-Str. 1, 09596 Freiberg, Germany.. Tel.: +49 3731 39 2484; fax: +49 3731 39 3638.
E-mail addresses: conny.zeeb@gmail.com, conny.zeeb@ifgt.tu-freiberg.de.(C. Zeeb)

0098-3004/$ - see front matter © 2013 Elsevier Ltd. All rights reserved.
http://dx.doi.org/10.1016/j.cageo.2013.04.027

behaviour using numerical simulations. The outcome of these simulations is normally a 2D or 3D permeability tensor, which can be used for the subsequent upscaling of the fracture network hydraulic properties in an equivalent porous media (EPM) (e.g. Bernard, 2002; Blum et al., 2005; Bodin et al., 2007; FracMan7, 2012). A typical way to acquire the data required for the generation of artificial DFN involves time-consuming and tedious manual measurements from outcrops or well cores. Recent developments in the automatic detection of lineaments from aerial photographs and satellite images (e.g. Masoud and Koike, 2011), the LIDAR technology (e.g. Wilson et al., 2011) and televiewer imaging of boreholes (e.g. Spillmann et al., 2007) provide time-efficient methods to acquire large quantities of fracture data. However, the information obtained by these methods should be cross-checked by local manual measurements and/or ground truthing to distinguish between true and false discontinuities (e.g. goat tracks), which could be interpreted as a lineament on a satellite image or aerial photograph.

Some of the programs that are used to process the information acquired by LIDAR and borehole televiewer measurements also provide basic tools for the analysis of fracture lengths and strike (e.g. Masoud and Koike, 2011; FracMan7, 2012). Programs specifically designed for the analysis of fracture data are often better suited. The open-access codes LINDENS (Casas et al., 2000) and SAL (Ekneligoda and Henkel, 2010) use the coordinates of fracture endpoints, for example from GIS analysis (e.g. Holland et al., 2009a), as inputs. Both programs analyze fracture length and orientation using frequency histograms and rose diagrams. The first one provides information on fracture density, whereas the second one focuses on additional spatial properties such as fracture spacing and unidirectional frequency. Markovaara-Koivisto and Laine (2012) provide a MATLAB script for the analysis and visualization of scanline data. The software package FracSim3D (Xu and Dowd, 2010) is in fact a fracture network generator, but also incorporates scanline, window and planar methods to sample fracture network characteristics from the generated networks. FracSim3D also offers statistical tools including histogram analysis, probability plots, rose diagrams and hemispherical projections (Xu and Dowd, 2010). Since statistical analysis by histograms and probability plots strongly depend on the binning of the data (e.g. Bonnet et al., 2001), the cumulative distribution function (cdf) is used in FraNEP to analyze fracture lengths. Though numerous other programs are available for the evaluation of fracture data, a complete review of them is beyond the scope of the current work. Nevertheless, the given examples illustrate well that such programs are often developed for a specific study. Moreover, to our knowledge, no open-access software provides a comprehensive and complete analysis, which includes all three typical sampling methods for the analysis of fracture networks.

The objective of the current study is therefore to provide such a program. FraNEP (Fracture Network Evaluation Program) was developed to quickly evaluate large amounts of fracture data, thus closing the gap between the automatic detection of lineaments and DFN modelling. For input the fractures have to be defined by their endpoint coordinates. Complementary information about the dimension of the study area and fracture sets support fracture network analysis. The statistical characteristics of a fracture network can be evaluated by applying the scanline sampling, the window sampling or the circular estimator method. The results of the analysis provide information on: (a) single fracture characteristics, such as fracture length and strike, (b) fracture network characteristics, like fracture density, intensity, mean length and length distribution, and (c) censoring bias. FraNEP was specifically developed in Visual Basic for Applications for Microsoft Excel™, which makes the program easy-to-use and enables a post-processing of the results without the need to export them to other software.

In the following sections we provide information and references for the theory behind sampling methods, correction techniques and data analysis in FraNEP. The data required for input, the definitions of the sampling process and the options that allow adopting the program to personal preferences are described in detail. Finally, a study area from the Oman Mountains is used to illustrate the application of FraNEP.

2. Background

2.1. Sampling methods

The following chapter briefly describes the three main sampling methods (scanline, window sampling and circular estimator) and the main biases typically related to the sampling process. A summary of governing equations used to calculate fracture density, intensity and mean length are presented in Table 1.

The scanline sampling method evaluates the characteristics of the fracture network based on the collection of data using all fractures intersecting with a sampling line (e.g. Priest and Hudson, 1981). This method allows a quick analysis of fracture network characteristics on outcrops and is the most widely used method for subsurface analysis (e.g. borehole image-logs and cores). A scanline survey can be used to measure parameters of individual fractures (e.g. orientation, length and aperture) and to calculate 1-dimensional information of fracture networks, such as linear fracture intensity (Table 1). Scanline measurements can be affected by (a) orientation bias (e.g. Terzaghi, 1965; Lacazette 1991; Priest,

Table 1
Definitions and governing equations of fracture density (p), intensity (I) and mean length (l_m) for the scanline sampling, window sampling and circular estimator methods. The latter is based on Rohrbaugh et al. (2002).

Parameter	Definition		Scanline sampling	Window sampling	Circular estimator
Density (p)	Areal	Number of fractures per unit area [L^{-2}]	–	$p=\frac{N}{A}$	$p=\frac{m}{2\pi r^2}$
Intensity (I)	Linear[a]	Number of fractures per unit length [L^{-1}]	$I=\frac{N}{L}$	–	–
	Areal	Fracture length per unit area [$L\times L^{-2}$]	–	$I=\frac{\sum l}{A}$	$I=\frac{n}{4r}$
Mean length (l_m)		Mean fracture length [L]	$l_m=\frac{\sum l}{N}$	$l_m=\frac{\sum l}{N}$	$l_m=\frac{\pi r}{2}\frac{n}{m}$

L is an arbitrary unit of length, N is the total number of sampled fractures, SL is the scanline length, A is the sampling area, r is the radius of the circular scanline, l is the fracture length, n and m are the number of intersections with a circular scanline and the number of endpoints in a circular window enclosed by the circular scanline.

[a] Also often referred to as fracture frequency.

1993), (b) size bias (e.g. Priest, 1993; Bonnet et al., 2001; LaPointe (2002); Manzocchi et al., 2009), (c) truncation bias (e.g. Bonnet et al., 2001; Pérez-Claros et al., 2002; Roy et al., 2007) and (d) censoring bias (e.g. Priest, 1993, 2004; Pickering et al., 1995; Riley, 2005). There are several techniques available to correct these biases (Section 2.2).

The window sampling method evaluates the characteristics by considering all fractures present within a selected sampling area (e.g. Pahl, 1981). The method is typically used for the analysis of outcropping subsurface analogues (e.g. Belayneh et al., 2009). It can be applied either directly on the ground or to aerial photographs and satellite images (e.g. Becker, 2006; Zeeb et al., 2010). Similar to the scanline method, the window sampling method can be used to measure parameters of individual fractures. However, window sampling provides 2-dimensional information of fracture networks such as fracture density (Table 1). Measurements can be affected by (a) orientation bias, (b) truncation bias and (c) censoring bias.

The circular estimator method uses a combination of circular scanlines and windows. The method is a maximum likelihood estimator (Lyman, 2003) and therefore it is not subject to sampling biases (Mauldon et al., 2001). Instead of directly sampling individual fractures, network parameters are estimated using statistical models (e.g. Mauldon et al., 2001). The method provides estimates of fracture density, intensity and mean length by counting the number of intersections (n) between fractures and a circular scanline, as well as the number of fracture endpoints (m) located within the area defined by this scanline (Table 1). According to Rohrbaugh et al. (2002) a minimum of ten circular scanlines should be placed in a sampling area with a radius exceeding the fracture spacing/block size, but considerable smaller than the extension of the area. In addition, more than 30 endpoints should be sampled (Rohrbaugh et al., 2002).

2.2. Correction techniques

In this section the correction techniques for sampling biases are described. The orientation bias of scanline surveys is automatically corrected by applying the Terzaghi correction (Terzaghi, 1965; Priest, 1993):

$$S = S_A \times \cos\,\theta \tag{1}$$

where S is the true mean spacing of fractures in a set, S_A is the apparent mean spacing of fractures in a set and θ is the acute angle between the scanline and the normal to fractures of a set. Linear fracture intensity (Table 1) is equal to $1/S$. Orientation bias can be minimized by placing a scanline parallel to the normal of a fracture set, such that θ is close to 0°. Additional scanlines should be used to acquire the fracture network data, if one scanline is not enough to capture all fracture sets (Priest, 1993).

Size bias is related to scanline sampling. The probability of a fracture intersecting with a scanline is proportional to the fracture length. Therefore, short fractures are underrepresented in the fracture length measurements acquired by scanline sampling, which causes an overestimation of fracture mean length and wrong estimates of fracture length distributions. Possible correction techniques for size bias are described by, for example, Bonnet et al. (2001), LaPointe (2002) and Zeeb et al. (in press).

Truncation bias is caused by the resolution limitations of an observation device (e.g. satellite image, human eye, hand lenses or microscope). Fractures with a size (length or width) below a certain value, which depends on the used observation device, are not detectable. Moreover, as fracture size approaches this detection limit, fewer fractures are recognized. In a log–log plot of fracture size versus cumulative number, this effect causes a flattening of the plotted data curve towards small fracture sizes. A possible correction technique is the application of the chord method (Pérez-Claros et al., 2002; Roy et al., 2007; Zeeb et al., in press).

Censoring bias is typically related to the presence of eroded or altered parts of the sampling area, the vegetation coverage or the presence of overlaying rock layers (e.g. Priest, 1993; Pickering et al., 1995). Censoring bias often causes an overestimation of fracture density (e.g. Kulatilake and Wu, 1984; Mauldon et al., 2001). Only fractures with their centre inside a sampling area should be included when calculating fracture density. In order to know the relative lengths of censored fractures and to correct for censoring bias, the exact fracture length distribution needs to be known (e.g. Priest, 2004; Riley, 2005). Since the underlying distribution of fracture lengths is generally unknown, it is difficult to ascertain whether a fracture center is inside the sampling area or not (Mauldon, 1998). This author uses the principle of associated endpoints to calculate an unbiased fracture density, which is also implemented in the circular estimator method (Mauldon et al., 2001). For window sampling an optional correction technique ("*Fracture density*") is available to reduce the overestimation of fracture density. The technique is based on the assumption that 50% of the censored fractures have more than half of their length, and thus also their centre, outside the selected sampling area. Applying this simple rule significantly reduces the typical

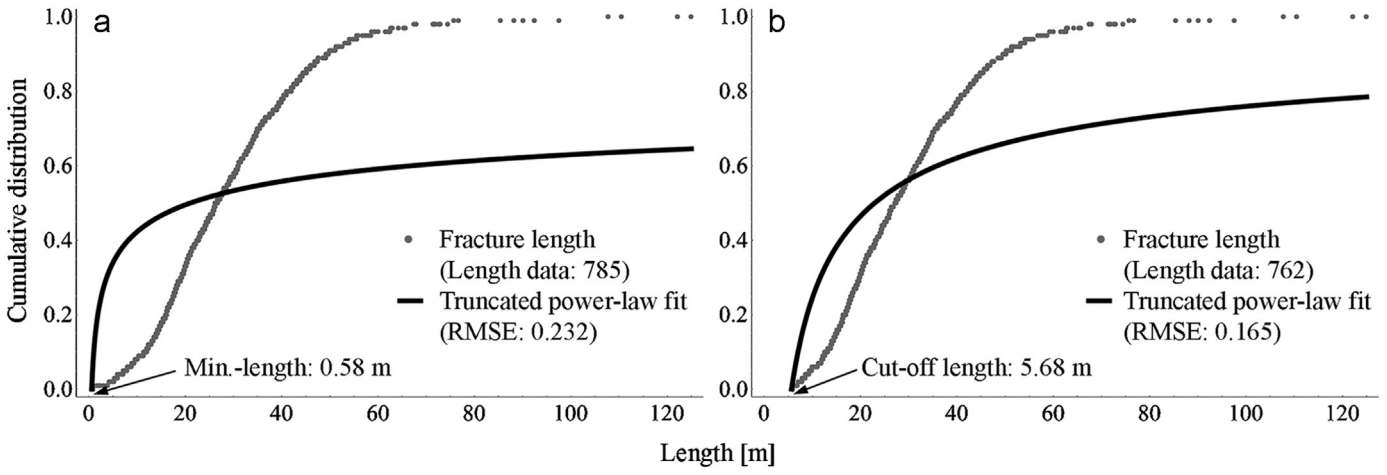

Fig. 1. Example for the correction of artificial censoring bias applying the "*Lower uncensored cut-off length*" option. Plotted is the cumulative distribution of the fracture lengths measured by application of the window sampling method to the field example (see below, Section 4) and the fitted cumulative distribution function of a truncated power-law (Eq. (2)). (a) shows the fit for all fracture lengths and (b) the fit excluding the fracture lengths below the lower uncensored cut-off length of 5.68 m.

overestimate and provides results closer to the true fracture density (Zeeb et al., in press). Note that this technique does not correct censoring bias per se, but instead reduces the trend in overestimating fracture density with increasing censoring bias.

An additional bias induced by the application of the window sampling method (see Section 3.2) is the artificial censoring bias. Fractures intersecting the boundaries of a sampling area become artificially censored. This can result in extremely short fracture lengths (Fig. 1a), which strongly influence the resulting length distribution. Although the impact on the best-fit distribution is relatively small or even negligible for lognormal or exponential distributions, it has a significant influence if the distribution is power-law (Eq. (2)). An optional correction technique ("*Lower uncensored cut-off length*") can be applied to neglect all fractures with lengths below the shortest uncensored fracture. The fracture lengths measured by the application of the window sampling to the field example are used to illustrate the effect of the correction technique on a truncated power-law fit. The fitting accuracy increases significantly, when all lengths below the lower uncensored cut-off length are neglected for the evaluation of the length distribution (Fig. 1b).

2.3. Analysis of fracture lengths

The length distribution of fractures is analysed using their cumulative distribution. Three equations are currently provided to describe the fracture length distribution: (1) truncated power-law (Eq. (2)), (2) lognormal (Eq. (3)) and (3) exponential (Eq. (4)). Although other distributions can also be found, these are the most commonly observed (e.g. Odling et al., 1999; Bonnet et al., 2001). Power-law relationships are often used to describe the distribution of fracture parameters such as length and aperture (e.g. Bonnet et al., 2001). The cumulative distribution function of a truncated power-law is given by Blum et al. (2005) and Riley (2005):

$$f(l) = 1 - \left(\frac{l}{l_0}\right)^{-E} \tag{2}$$

where l is the fracture length, l_0 is the shortest observed fracture length and E is the power-law exponent. The lognormal distribution is also commonly used to describe fracture lengths (Priest and Hudson, 1981). Resolution effects (i.e. truncation bias) or the presence of a characteristic scale, for example associated to lithological layering, imposed on power-law distributed length data can give rise to lognormal distributions (Odling et al., 1999; Bonnet et al., 2001). The cumulative distribution function of a lognormal distribution is given by Priest and Hudson (1981):

$$f(l) = 0.5 + 0.5Erf\left(\frac{Ln(l) - \mu}{\sqrt{2\sigma^2}}\right) \tag{3}$$

where μ and σ are the mean and the standard deviation of the natural logarithm of l. Fracture lengths are best described by an exponential distribution when fractures are formed as a result of fracture growth under a uniform stress state (Dershowitz and Einstein, 1988) or are developed at early stages of deformation (Bonnet et al., 2001). The cumulative distribution function of an exponential distribution is provided by Cruden (1977):

$$f(l) = 1 - e^{-\lambda l} \tag{4}$$

where λ is the rate parameter. The user can apply one of above distributions to the fracture length data or allow FraNEP to determine the best-fitting length distribution automatically.

The accuracy of the best fit is indicated by (1) the root mean squared error (RMSE) (Eq. (5)), (2) the sum of squared errors (SSE) (Eq. (6)) and (3) the maximum squared error (MSE) (Eq. (7)) (Loague and Green, 1991). The RMSE is given by:

$$\mathrm{RMSE} = \sqrt{\sum_{i=1}^{N} (P_i - O_i)^2 / N} \tag{5}$$

where n is the total number of measurements, P is the predicted/calculated value and O is the observed/measured value. The RMSE is commonly used to compare the best fits of different data. The SSE is a simplification of the RMSE and is given by:

$$\mathrm{SSE} = \sum_{i=1}^{N} (P_i - O_i)^2 \tag{6}$$

For the automatic evaluation of the best fit the SSE is used, which is valid since the three distribution functions (Eqs. (2)–(4)) are fitted to the same data. The MSE is given by:

$$\mathrm{MSE} = (P_i - O_i)^2 |_{i=1}^{N} \tag{7}$$

3. Program description

The methodology used to evaluate the characteristics of a fracture network based on trace-line maps is divided in three main steps: (I) data input, (II) sampling and (III) options for the analysis (Fig. 2).

3.1. Step I: Input

The following information is required as program inputs: (1) endpoint coordinates of each fracture, (2) number of fracture sets as well as their strike spread (minimum and maximum value) and (3) dimension of the study area (Fig. 2; Fig. 3; Table 2). Endpoint coordinates are imported as points with coordinates (X1, Y1) and (X2, Y2). The length and strike of each fracture are automatically calculated using these two points. Summing up all lengths and dividing this total fracture length by the total number of fractures provides a first estimate of mean fracture length (Fig. 2; Table 2). Once the different fracture sets are defined, we automatically get the mean strike and the number of fractures for each set (Fig. 2; Table 2). If the definition of fracture sets is unclear, the input data can also be treated as one single set with strikes that range from 0° to 180°. The position and size of the study area is defined by the coordinates of its lower-left corner and the extension in the X- and Y-directions. Area size, fracture density and fracture intensity are calculated once the study area is defined (Fig. 2; Table 2). A definition of the study area is not necessarily required and can be skipped, if the size of the study area is unknown, or if data are missing from parts of the area, for example due to erosion, vegetation cover or surface alteration. The preliminary results calculated for fracture mean length, density and intensity should be always treated carefully.

FraNEP includes the possibility of generating and displaying a trace-line map from the imported fractures. To distinguish between different sets of fractures their strikes can be analyzed using a rose diagram plot, which is generated together with the aforementioned trace-line map. The rose diagram can be drawn with or without fracture-length weighting.

3.2. Step II: Sampling

Three sampling methods can be applied to evaluate the characteristics of a fracture network: (1) scanline sampling, (2) window sampling and (3) circular estimator. A scanline is defined by the coordinates of its start- and endpoints (Fig. 4). The sampling areas for the application of the window sampling and circular estimator methods are selected by defining a point of origin (lower left corner) and the extension of the area in X- and Y-

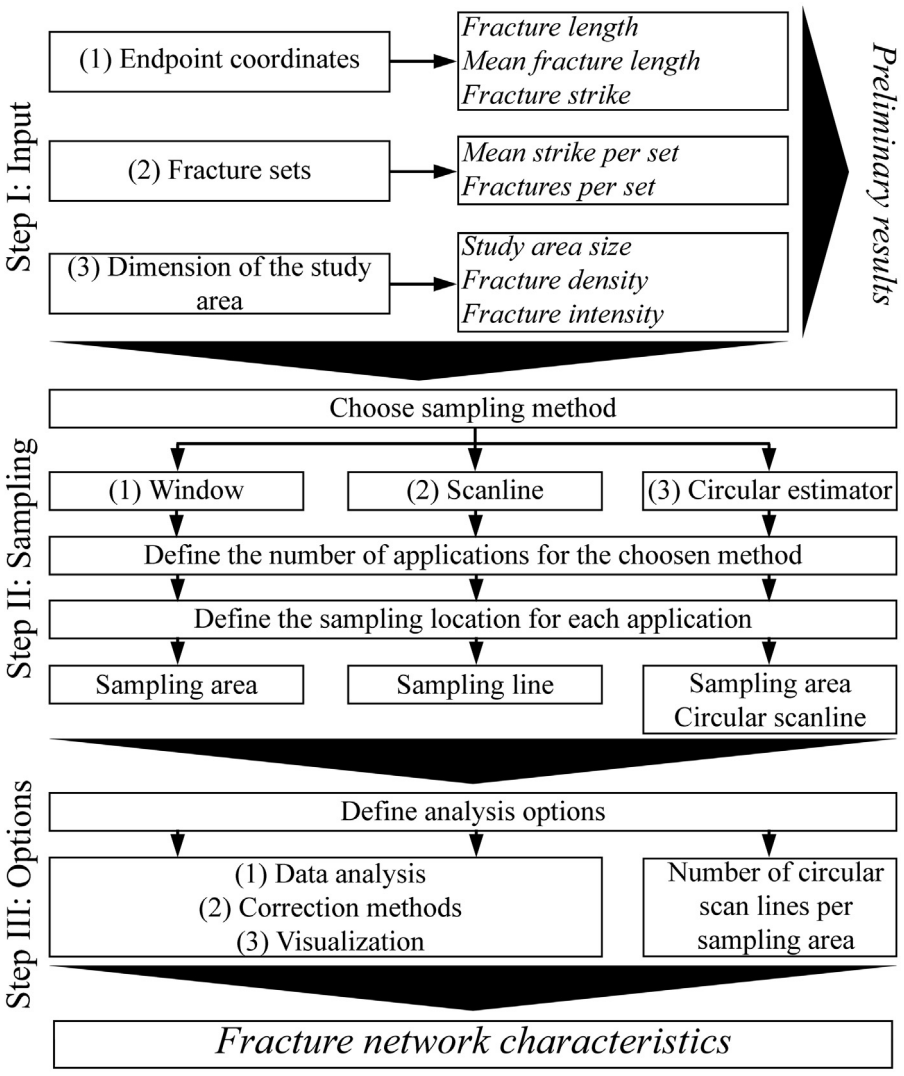

Fig. 2. Schematic methodology to evaluate the fracture-network characteristics using trace-line maps (*Italics* indicate results).

	A	B	C	D	E	F	G	H	I	J	K	L	M
1	x1	y1	x2	y2	Strike [°]	Length [L]		**Fracture sets**	3				
2	518114.27	2564287.26	518332.16	2564315.05	82.7	219.6		Strike [°]	Set1	Set2	Set3	Set4	
3	517902.58	2564405.77	517826.68	2564523.89	147.3	140.4		Min	10	100	155	0	
4	518089.13	2564676.55	518220.21	2564682.14	87.6	131.2		Max	100	155	10	0	
5	518010.48	2564478.30	517897.45	2564524.71	112.3	122.2		Mean	68.9	133.4	178.4	-	Sum
6	518402.83	2564399.18	518327.77	2564495.20	142.0	121.9		Fractures per set [-]	294	770	172	0	1236
7	518195.95	2564580.11	518120.25	2564670.65	140.1	118.0							
8	518410.00	2564396.64	518338.49	2564486.91	141.6	115.2		**Dimensions of study area**					
9	518316.18	2564553.89	518205.85	2564561.31	93.8	110.6		Point of Origin	X-dir	517760			
10	518201.04	2564535.17	518308.27	2564546.38	84.0	107.8			Y-dir	2564285	Visualize		
11	517878.39	2564433.28	517793.94	2564486.89	122.4	100.0		Window Size	X-dir	650			
12	518380.41	2564405.03	518319.97	2564482.53	142.1	98.3			Y-dir	405			
13	518393.57	2564465.96	518331.67	2564541.02	140.5	97.3		Scaling		0.5			
14	517911.20	2564544.48	517825.67	2564587.89	116.9	95.9		Rose diagram	2	5			
15	518387.24	2564441.10	518326.31	2564511.29	139.0	92.9		**Preliminary results**					
16	518211.27	2564414.58	518125.48	2564449.19	112.0	92.5		Number of fractures [-]	1236				
17	517973.95	2564450.79	518066.35	2564455.09	87.3	92.5		Sampling area size [L²]	263250				
18	517837.59	2564375.88	517760.00	2564423.73	121.7	91.2		Fracture density [L^{-2}]	0.005				
19	518172.07	2564532.02	518117.49	2564603.79	142.7	90.2		Fracture intensity [L L^{-2}]	0.15				
20	517998.87	2564616.26	518086.98	2564611.53	93.1	88.2		Mean fracture length [L]	31.3				

Fig. 3. Illustration of the "Input" worksheet. Columns "A"–"B" contain the endpoint coordinates of each fracture and columns "E" and "F" its automatically calculated strike and length. The highlighted section "Fracture sets" and "Dimension of study area" are reserved for the definition of different fracture sets and the studied area, respectively. The section "Preliminary results" provides first estimates for fracture density, intensity and mean length. The "Visualize"-button can be used to generate a trace-line map and a rose diagram plot.

Table 2
Input data and governing equations for the calculation of individual fracture and the preliminary fracture network characteristics (Fig. 2; Fig. 3).

Input		Parameter	Equation
Endpoint coordinates			
$(X1_i, Y1_i)$		Length, l_i [L]	$l_i = \sqrt{(X2_i - X1_i)^2 + (Y2_i - Y1_i)^2}$
$(X2_i, Y2_i)$		Mean length, l_m [L]	$l_m = \frac{1}{N}\sum_{i=1}^{N} l_i$
		Strike, O_i [°]	$O_i = \tan^{-1}\left(\frac{X1_i - X2_i}{Y1_i - Y2_i}\right)\ 0° \le O_i \le 180°$
Fracture sets			
Set j	$O^j_{min} \le O_i < O^j_{max}$	Mean strike, O^j_m [°]	$O^j_m = \frac{1}{N}\sum_{i=1}^{N} O_i$
		Fractures per set, N_j [−]	$N_j = \sum_{i=1}^{N} o_i$
Dimension of the study area			
Point of origin (X, Y)		Study area size, A [L^2]	$A = X_{dir} \times Y_{dir}$
Extension (X-dir, Y-dir)		Fracture density, p [L^{-2}]	$p = \frac{N}{A}$
		Fracture intensity, I [$L \times L^{-2}$]	$I = \frac{\sum_{i=1}^{N} l_i}{A}$

i denotes individual fractures, j denotes different fracture sets and L is an arbitrary unit of length.

	A	B	C	D	E	F	G	H	I	J	K	L	M	N	O	P
1		Window sampling					Scanline sampling						Circular estimator			
2	Analysis	Point of origin		Window size		Area [L²]	Start		End		Length [L]	Scanline strike [°]	Centre		Radius	Area [L²]
3		X	Y	X-dir	Y-dir		X	Y	X	Y			X	Y		
4	1	517835	2564355	500	300	150000.0	517835	2564355	518335	2564655	583.1	59.0			35	3848.5
5	2					0.0					0.0	180.0				0.0
6	3					0.0					0.0	180.0				0.0
7	4					0.0					0.0	180.0				0.0

Fig. 4. Illustration of the "Sampling" worksheet. Columns "B"–"E" are used to define the sampling areas required for the window sampling and circular estimator methods. "G"–"J" allow the definition of endpoint coordinates required for the scanline sampling method. "M"–"O" are reserved for the centre and radius of circular scanlines used by the circular estimator method.

directions (Fig. 4). Fractures intersecting a boundary of the selected sampling area are considered censored and the intersection point is used to calculate the length of the censored fracture. The circular scanlines used by the circular estimator method are defined by their centres and radii (Fig. 4). Centres for circular scanlines are defined by their X- and Y-coordinates and can be placed either manually or randomly. The distance between the boundaries of a sampling area and the centres is equal to the radius plus a small constant value of 0.1 to avoid interaction between scanlines and boundaries. Sampling areas and/or scanlines can be placed anywhere within the study area. Although we apply each sampling method to the example study area only once, it is also possible to simultaneously apply up to 200 sampling areas/lines. The fracture network characteristics evaluated by the application of the window and scanline sampling methods are summarized in an extra worksheet for each analysis. Furthermore, the lengths, strikes and endpoints of the sampled fractures are provided in this worksheet. Since the circular estimator provides no information on fracture lengths and strike, the fracture network characteristics of all analyses are summarized in one worksheet.

3.3. Step III: Options

Three categories of options are available for the characterization of a fracture network. These options can be used to select (1) the correction methods, (2) the analysis performed with the acquired data and (3) the visualization of results (Fig. 5, Table 3).

3.3.1. Correction methods

The option "*Fracture density*" accounts for fractures, which are only partly visible and therefore censored. The option applies a simple routine to reduce the overestimation of fracture density using window sampling by neglecting half of the censored fractures during the calculation.

The option "*Lower uncensored cut-off' length* corrects artificial censoring bias. All fractures with lengths below the shortest uncensored fracture are neglected to reduce the impact of artificially censored fractures on the evaluation of the length distribution.

3.3.2. Data analysis

The option "*Length fit*" must be chosen, if the user wants to evaluate the length distribution of a fracture network. The user can either manually apply one of the three provided distributions (truncated power-law, lognormal or exponential) to the fracture length data or allow FraNEP to evaluate the best fitting length distribution automatically.

The option "*Circular scanlines*" defines the number of circular scanlines applied to a sampling area. Rohrbaugh et al. (2002) suggested that a minimum of ten scanlines should be used to characterize a fracture network with the circular estimator method.

3.3.3. Visualization

The option "*Diagram type*" allows the visualization of the sampled fracture lengths as (a) a plot of the cumulative distribution and/or (b) a log–log plot of the cumulative number. Note that for the evaluation of the length distribution, the cumulative distribution is used.

The option "*Scanline combination*" joins the results from two consecutive and/or all applied scanlines.

The option "*Write strikes*" allows the reduction of computational times. This option can be used to skip the evaluation of fracture

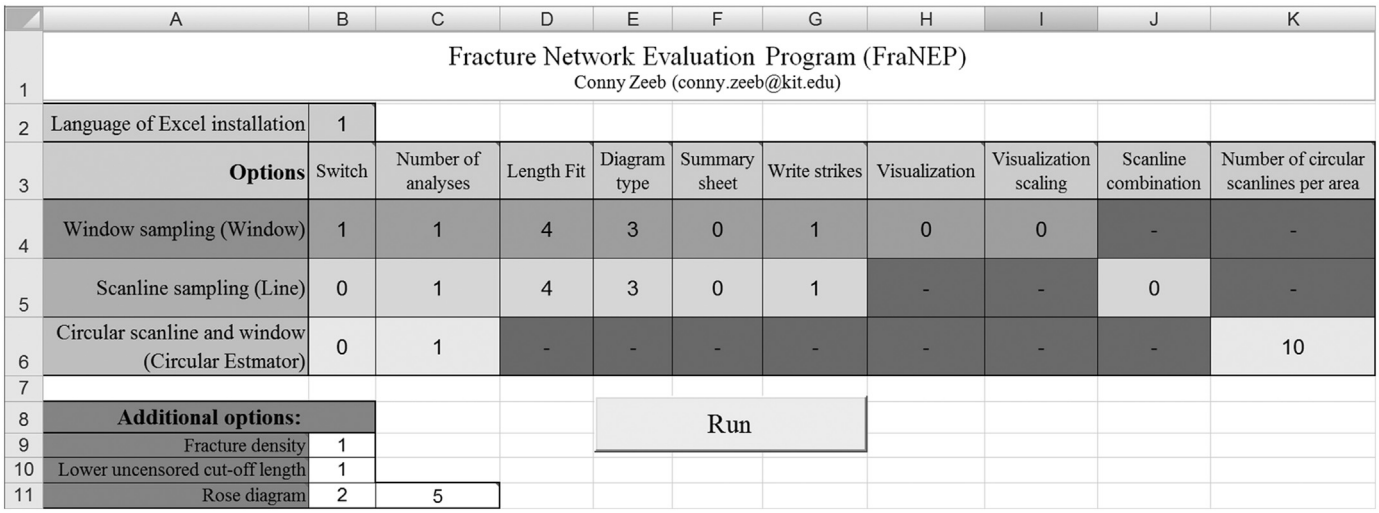

	A	B	C	D	E	F	G	H	I	J	K
1	Fracture Network Evaluation Program (FraNEP) Conny Zeeb (conny.zeeb@kit.edu)										
2	Language of Excel installation	1									
3	**Options**	Switch	Number of analyses	Length Fit	Diagram type	Summary sheet	Write strikes	Visualization	Visualization scaling	Scanline combination	Number of circular scanlines per area
4	Window sampling (Window)	1	1	4	3	0	1	0	0	-	-
5	Scanline sampling (Line)	0	1	4	3	0	1	-	-	0	-
6	Circular scanline and window (Circular Estmator)	0	1	-	-	-	-	-	-	-	10
7											
8	**Additional options:**				Run						
9	Fracture density	1									
10	Lower uncensored cut-off length	1									
11	Rose diagram	2	5								

Fig. 5. Illustration of the "Options"-worksheet. Dark gray cells marked by "–" indicate options that are not applicable for this sampling method.

Table 3
Options for (1) correction methods, (2) data analysis and (3) visualization of results. The symbols "+" and "–" indicate whether an option is applicable to the chosen sampling method or not.

Category	Option	Description	Window	Scanline	Circular estimator
(1) Correction methods	Fracture density	Reduces the overestimation of fracture density	+	–	–
	Lower uncensored cut-off length	Corrects artificial censoring bias	+	+	–
(2) Data analysis	Length fit	Defines the fitting for fracture lengths	+	+	–
	Circular scanlines	Defines the total number of circular scanlines placed in each sampling area	–	–	+
(3) Visualization	Diagram type	Creates a plot of sampled fracture lengths	+	+	–
	Scanline combination	Combines the results from two and/or all scanlines	–	+	–
	Write strikes	Write strikes in the output-sheets	+	+	–
	Rose diagram	Plots the fracture strikes in a rose diagram	+	+	–
	Visualization	Creates a trace-line map of the sampled fractures	+	–	–

strikes, thus reducing the calculation time required for the analysis of large data sets.

The option "*Rose diagram*" creates a plot of fracture strikes in the form of a rose diagram with an adaptable bin size. A new worksheet is added for the data preparation and the visualization of the rose diagram. The plot shows the cumulative number or the sum of fracture lengths per bin.

The "*Visualization option*" creates a trace-line map of the fractures in the area analyzed by the window sampling method. The map is created in a new worksheet and a scaling coefficient is used to change the size of the map.

4. Example of application: Fracture networks in Jabal Akhdar (Oman)

A field case example from the Oman Mountains, which was already studied by Holland et al. (2009a), is used to illustrate the methodology of FraNEP. The study area is located at the southern flank of the Jabal Akhdar dome, the most prominent structure of the Oman Mountains (Fig. 6) (Glennie et al., 1973; Breton et al., 2004). The exposed rocks are mainly Mesozoic limestones with interbedded shales and marly layers, which were deposited on the southern Neothetyan continental margin from late Jurassic to upper Cretaceous times (Glennie et al., 1973; Breton et al., 2004). Closure of the Neotethyan Ocean during the early Cretaceous led to SSW directed obduction of the Semail Ophiolite and the volcano-sedimentary Hawasina nappes over the autochthonous carbonates (Glennie et al., 1973; Breton et al., 2004). Uplift and exhumation of the autochthonous carbonates and the formation of the Jabal Akhdar tectonic window is related to the development of the Makran subduction zone during the Tertiary and still ongoing (Breton et al., 2004). The complex geological history of the rocks is reflected by numerous sets of discontinuities, including faults of different sizes, fractures, veins, stylolites, bedding parallel slip surfaces and joints (e.g. Hilgers et al., 2006; Holland et al., 2009a; 2009b).

The available input data consists of a polyline shape file, which contains approximately 157,000 lineaments identified by manual interpretation of a Quickbird satellite image with a panchromatic resolution of 0.7 m (Holland et al., 2009b). The study area investigated here is a small part of this shape file and contains a total of 1236 lineaments. These lineaments correspond to veins, fractures and joints measured from an outcrop surface. Extensive ground truthing revealed that the vast majority of the interpreted lineaments belong to a recent generation of joints. These joints were widened by erosion and filled with bright alluvium creating a good optical contrast to the dark grey carbonate rocks. Here we

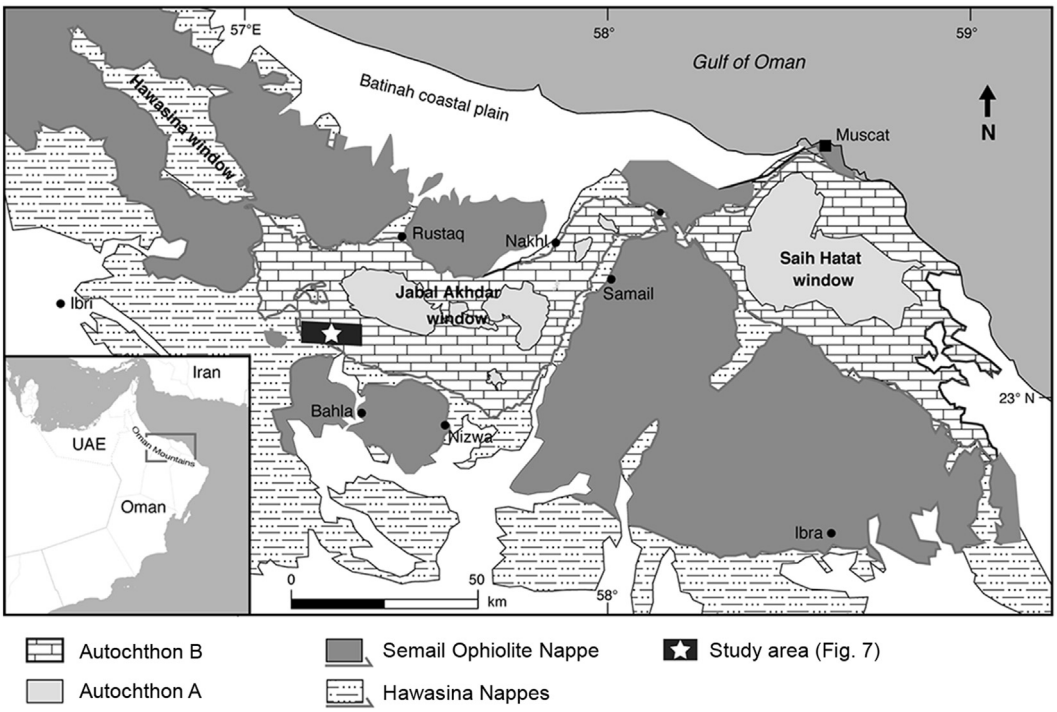

Fig. 6. Overview of the geology in the Oman Mountains and location of the study area in Fig. 7 (modified from Breton et al., 2004).

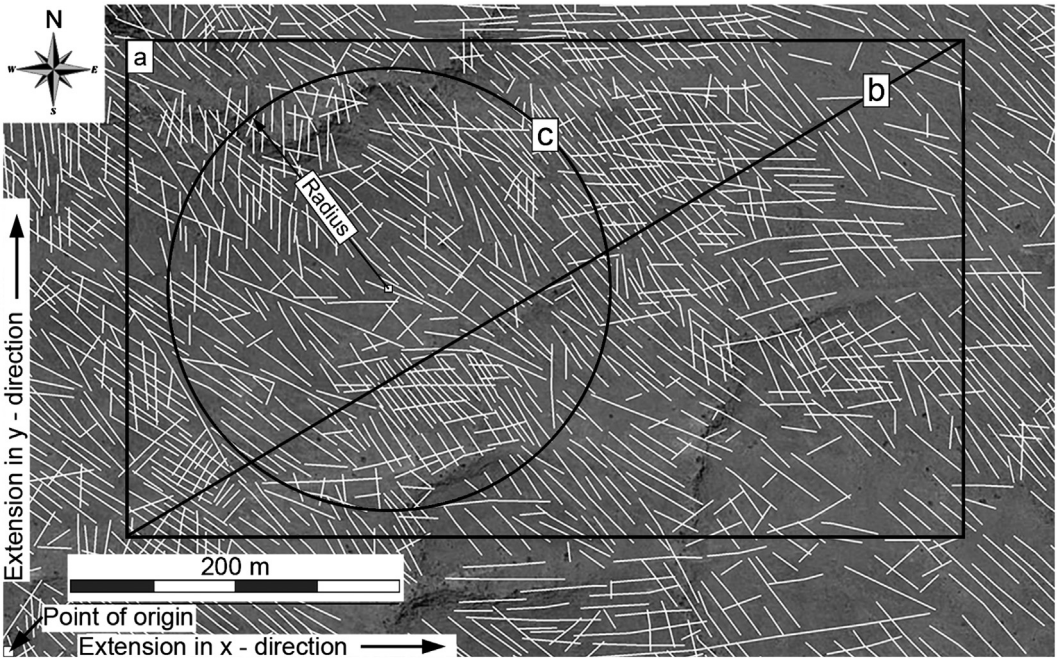

Fig. 7. Satellite image (modified from Google, GeoEye) and size of the study area at the southern flank of the Jabal Akhdar dome in the Oman Mountains (Holland et al., 2009b). Lineaments identified by manual interpretation are represented by white lines. (a) Sampling area analysed using the window sampling and circular estimator method, (b) sampling line analysed using the scanline sampling method and (c) example of a circular scanline. The UTM coordinates of the lower left corner are 40N 517744 2564259.

use the general term fractures, when referring to these lineament data, even if most of them are in fact joints.

4.1. Input data and sampling

The endpoints of the fractures from the field example (Fig. 7) are given as UTM coordinates, which are imported to FraNEP. From the input the lengths and strikes of individual fractures are calculated, as well as a first estimate of mean fracture length (Table 4). Using the length-weighted rose diagram of the fracture strikes (Fig. 8), three main fracture sets can be identified. The spread of strikes as well as the mean strike and number of fractures per set are summarized in Table 4. The size of the study area and preliminary estimates of fracture density and intensity are also presented.

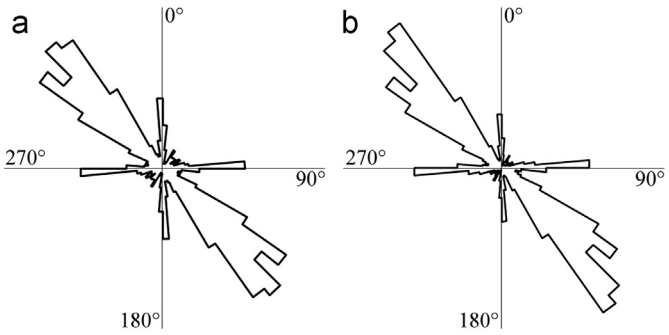

Fig. 8. Rose diagram (bin size of 5°) of the fracture strikes in Fig. 7, with (a) the cumulative-number plot and (b) the length-weighted plot.

4.2. Fracture network characteristics

In Fig. 7. the locations for the application of the window sampling (a), the scanline sampling (b), and the circular estimator (c) methods are shown. The definitions for the sampling areas and the scanline are summarized in Table 5 and a summary of the calculated fracture network characteristics in Table 6.

Fig. 9 shows the cumulative distribution of the fracture lengths sampled by the scanline and window methods. The fitted cumulative distribution functions and the fitting accuracy for a truncated power-law (Eq. (2)), a lognormal (Eq. (3)) and an exponential (Eq. (4)) function are also presented. For both sampling methods the best fit to the measured fracture lengths was found to follow a lognormal distribution. The strikes of the sampled fractures are

Table 4
Input and preliminary results for the fracture network at Jabal Akhdar (Oman), with one fracture ($i=1$) as an example for the calculation of fracture length and strike (Fig. 7).

Input		Parameter	Preliminary result	
Endpoint coordinates[a]				
$X1_1$: 517830	$Y1_1$: 2564405	Length, l_i	66.7 m	
$X2_1$: 517777	$Y2_1$: 2564445	Mean length, l_m	31.3 m	
		Strike, O_i	127.2°	
Fracture sets				
Set 1	$010° \le O_i < 100°$	Mean strike, O_m^j	Set 1	68.9°
			Set 2	133.4°
Set 2	$100° \le O_i < 155°$		Set 3	178.4°
Set 3	$155° \le O_i < 010°$	Fractures per set, N_j	Set 1	294
			Set 2	770
			Set 3	172
Dimension of the study area				
Point of origin (X, Y)[a]	517760 2564285	Study area size, A	2.63×10^5 m^2	
Extension (X-dir, Y-dir)	650 m 405 m	Fracture density, p	0.005 m^{-2}	
		Fracture intensity, l	0.15 m m^{-2}	

[a] UTM coordinates.

Table 5
Definition of the sampling areas/line locations for the application of the three sampling methods (Fig. 7).

Sampling method	Sampling location			
Window	Point of origin (X, Y)[a]		517835	2564355
	Extension (X-dir, Y-dir)		500 m	300 m
Scanline	Start point (X, Y)[a]		517835	2564355
	End point (X, Y)[a]		518335	2564655
Circular estimator	Sampling area	Point of origin (X, Y)[a]	517835	2564355
		Extension (X-dir, Y-dir)	500 m	300 m
	Coordinates centre (X, Y)		random	
	Radius		140 m	

[a] UTM coordinates.

Table 6
Fracture network characteristics of the Oman field example evaluated by the three sampling methods (Fig. 7). Fitted parameter 1 corresponds to E, μ or λ, and fitted parameter 2 to σ^2 (Eqs. 2–4).

Parameter		Window	Scanline	Circular
Sampled area [m²] or length of the scanline [m]		1.5×10^5	583	1.5×10^5
Number of fractures [−]		785	74	–
Fracture density [m^{-2}]		0.005	–	0.004
Fracture intensity [m m^{-2}] or fracture frequency (scanline) [m^{-1}]		0.15	0.13	0.17
Mean fracture length [m]		29.4	41.8	44.5
Number of censored fractures [−]		144	0	–
Number of fractures shorter than lower uncensored cut-off length [−]		23	0	–
Best fitted length distribution		lognormal	lognormal	–
Accuracy of the best fit	RMSE	0.014	0.053	–
	SSE	0.152	0.208	–
	MSE	0.001	0.011	–
Fitted parameter 1 (E, μ, λ)		$\mu=3.287$	$\mu=3.706$	–
Fitted parameter 2 (σ^2)		$\sigma^2=0.545$	$\sigma^2=0.384$	–

"–" Method provides no information.

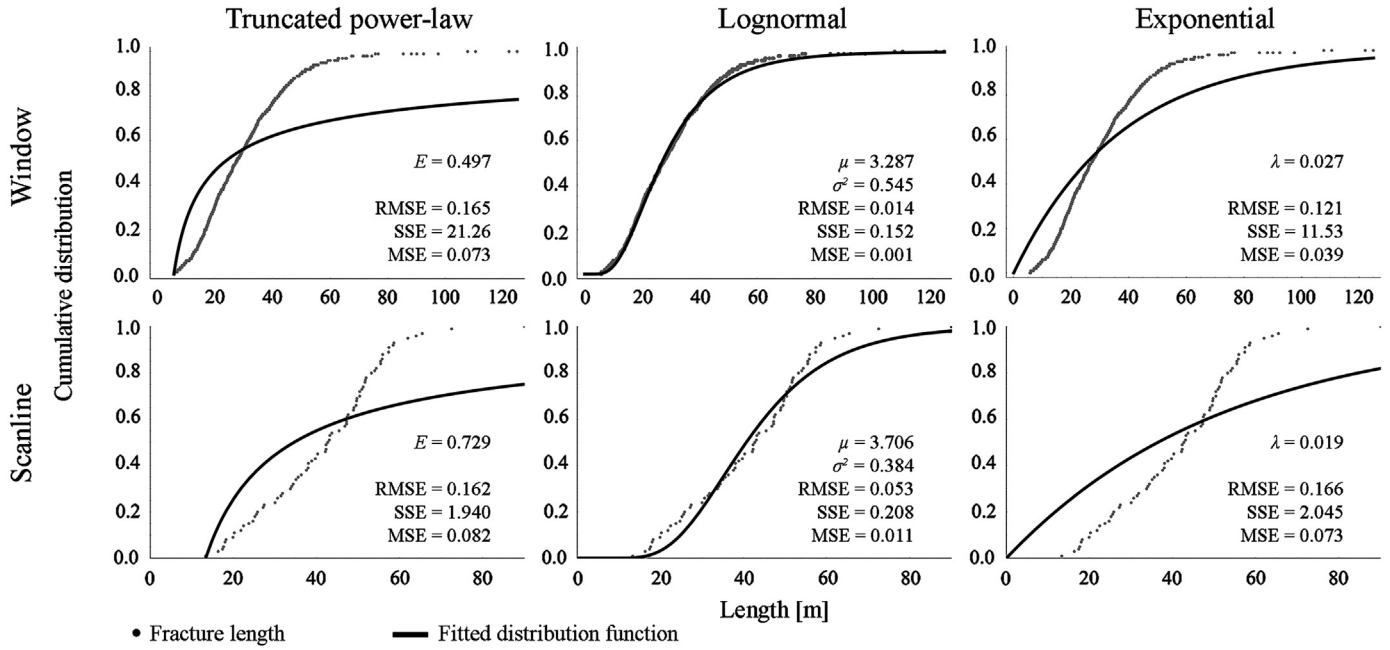

Fig. 9. Example illustrating the fit of a truncated power-law, lognormal and exponential function. Shown is the cumulative distribution of fracture lengths sampled by the scanline and window sampling methods. E, μ, σ^2 and λ are the fitted parameters of the corresponding distribution functions (Eqs. (2)–(4)). The accuracy of the fits is provided as RMSE, SSE and MSE.

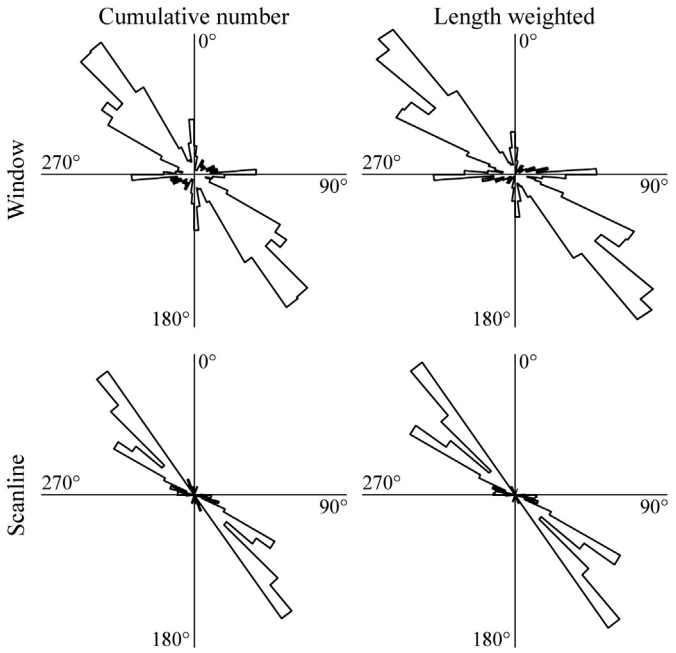

Fig. 10. Rose diagrams with a bin size of 5° showing the fracture strikes sampled by the scanline and window sampling methods.

presented as cumulative number and length-weighted rose diagrams in Fig. 10.

4.3. Discussion of the results

The fracture network characteristics obtained with the three sampling methods are dissimilar, especially the estimate of the mean fracture length (Table 6). One possible explanation lies in the sampling methods themselves. For example, the probability of a fracture to intersect with a scanline is proportional to its length, with an increasing probability for longer fractures. The underrepresentation of short fractures explains the differences between the window and scanline sampling methods in fracture intensity and mean length (e.g. Priest, 1993). Following the guideline of Rohrbaugh et al. (2002) for the application of the circular estimator method, we found that the radius of the circular scanlines should be at least 45 m for the current study. For this radius, values of fracture density are similar to those obtained from window sampling. In contrast, values for fracture intensity and mean length differed significantly from those obtained by window and scanline sampling. For example, estimates of mean fracture length were $\gg$100 m. Applying additional circular scanlines (up to 100) to the sampling area did not help to improve the results. Increasing the radii of the circular scanlines provided more reliable results. Therefore, we applied the circular estimator method with a radius of 140 m (Table 6). This approach provided values for fracture density, intensity and mean length closer to those of the other two sampling methods (Table 6). Although it would be highly interesting to compare the capability of the three sampling methods in more detail, this is beyond the scope of this study. A more detailed comparison of sampling methods is provided, for example, by Rohrbaugh et al. (2002), Weiss (2008) and Belayneh et al. (2009).

5. Conclusions

The presented software FraNEP automatically analyzes the statistical properties of 2D fracture networks based on trace-line maps. For the input, each fracture has to be defined by the coordinates of its endpoints. Techniques such as automatic lineament detection from satellite images or aerial photographs can provide such fracture data. For the evaluation of the network characteristics three commonly used sampling methods are available: (1) scanline sampling, (2) window sampling and (3) circular estimator. These methods can be applied to the entire study area or to specific sampling locations, if parts of the study area are obscured by erosion or vegetation. Hence, the most appropriate

sampling method can be used to evaluate the most representative part of a study area.

FraNEP provides the main network statistics, which include the length and strike of each fracture, estimates for fracture density, intensity, mean length and length distribution, and information on the number of censored fractures. Rose diagrams with adjustable strike bin size provide information on fracture strikes and allow a quick classification of fracture sets. The strikes in each bin can be plotted either as their cumulative number or by the sum of their fracture lengths. The evaluation of the fracture length distribution is done either automatically, or by choosing one of three distribution functions (truncated power-law, lognormal and/or exponential). Existing software often uses histograms and probability density plots to describe fracture length distributions. In FraNEP the cumulative distribution function is used to determine the best fit, to avoid problems related to binning.

FraNEP was specifically developed in Visual Basic for Applications in Microsoft Excel™, which makes the program easy-to-use and enables a post-processing of the results without the need to export them to other software. Moreover, the program code is organized in modules, which makes it easy to extend FraNEP to personal and site-specific requirements.

Other software packages, such as those presented in the introduction, or even manual analysis of the Jabal Akhdar study area would have yielded results similar to those obtained with FraNEP. However, different software packages would have been required to characterize fracture networks by means of different sampling methods, whereas a manual analysis would have been very tedious and time-consuming. The advantage of FraNEP is that it offers a complete and easy-to-use combination of characterization techniques and tools. A major novelty is that three commonly used sampling methods are combined into a single software package. Therefore, FraNEP is a time-efficient tool for the characterization of fracture networks.

Acknowledgements

This study was carried out within the framework of DGMK (German Society for Petroleum and Coal Science and Technology) research project 718 “Mineral Vein Dynamics Modelling”, which is funded by the companies ExxonMobil Production Deutschland GmbH, GDF SUEZ E&P Deutschland GmbH, RWE Dea AG and Wintershall Holding GmbH, within the basic research program of the WEG Wirtschaftsverband Erdöl- und Erdgasgewinnung e.V. We would like to acknowledge the companies for their financial support, their permission to publish these results and funding of the PhD grant to CZ and postdoctoral grant to EGR. We also would like to thank Franco Corona and Georg Schmitz from ExxonMobil Production Deutschland GmbH for their helpful advice. We are greatful to the helpful comments by the anonymous reviewers.

Appendix A. Supporting information

Supplementary data associated with this article can be found in the online version at http://dx.doi.org/10.1016/j.cageo.2013.04.027.

References

Becker, M.W., 2006. Potential for satellite remote sensing of ground water. Ground Water 44, 306–318, http://dx.doi.org/10.1111/j.1745-6584.2005.00123.x.

Belayneh, M.W., Matthäi, S.K., Blunt, M.J., Rogers, S.F., 2009. Comparison of deterministic with stochastic fracture models in water-flooding numerical simulations. AAPG Bulletin 93, 1633–1648, http://dx.doi.org/10.1306/07220909031.

Berkowitz, B., 2002. Characterizing flow and transport in fractured geological media: a review. Advances in Water Resources 25, 861–884, http://dx.doi.org/10.1016/S0309-1708(02)00042-8.

Bernard, S., 2002. Le logiciel MODFRAC: simulation de réseaux de fractures 2D et de l'écoulement associé (MODFRAC: a program for simulating steady-state flow in 2D random fracture networks). Geosciences DEA report (in French). University of Poitiers, France.

Blum, P., Mackay, R., Riley, M.S., Knight, J.L., 2005. Performance assessment of a nuclear waste repository: upscaling coupled hydro-mechanical properties for far-field transport analysis. Journal of Rock Mechanics and Mining Sciences 42, 781–792, http://dx.doi.org/10.1016/j.ijrmms.2005.03.015.

Blum, P., Mackay, R., Riley, M.S., 2009. Stochastic simulations of regional scale advective transport in fractured rock masses using block upscaled hydro-mechanical rock property data. Journal of Hydrology 369, 318–325, http://dx.doi.org/10.1016/j.jhydrol.2009.02.009.

Bodin, J., Porel, G., Delay, F., Ubertosi, F., Bernard, S., de Dreuzy, J.-R., 2007. Simulation and analysis of solute transport in 2D fracture/pipe networks: the SOLFRAC program. Journal of Contaminant Hydrology 89, 1–28, http://dx.doi.org/10.1016/j.jeonhyd.2006.07.005.

Bonnet, E., Bour, O., Odling, N.E., Davy, P., Main, I., Cowie, P., Berkowitz, B., 2001. Scaling of fracture systems in geological media. Reviews of Geophysics 39, 347–383, http://dx.doi.org/10.1029/1999RG000074.

Breton, J.-P., Béchennec, F., Le Métour, J., Moen-Maurel, L., Razin, P., 2004. Eoalpine (Cretaceous) evolution of the Oman Tethyan continental margin: insights from a structural field study in Jabal Akdhar (Oman mountains). GeoArabia 9, 1–18.

Casas, A.M., Cortés, A.L., Maestro, A., Soriano, M.A., Riaguas, A., Bernal, J., 2000. LINDENS: a program for lineament length and density analysis. Computers and Geosciences 26, 1011–1022, http://dx.doi.org/10.1016/S0098-3004(00)00017-0.

Cruden, D.M., 1977. Describing the size of discontinuities. International Journal of Rock Mechanics and Mining Sciences 14, 133–137, http://dx.doi.org/10.1016/0148-9062(77)90004-3.

Dershowitz, W.S., Einstein, H.H., 1988. Characterizing rock joint geometry with joint system models. Rock Mechanics and Rock Engineering 21, 21–51, http://dx.doi.org/10.1007/BF01019674.

Ekneligoda, T.C., Henkel, H., 2010. Interactive spatial analysis of lineaments. Computers and Geosciences 36, 1081–1090, http://dx.doi.org/10.1016/j.cageo.2010.01.009.

FracMan7, 2012. Golder Associates Inc., ⟨http://www.golder.com⟩.

Glennie, K.W., Boeuf, M.G.A., Hughes-Clarke, M.W., Moody-Stuart, M., Pilaar, W.F.H., Reinhardt, B.M., 1973. Late Cretaceous nappes in Oman Mountains and their geological evolution. AAPG Bulletin 57, 5–27.

Hilgers, C., Kirschner, D.L., Breton, J.-P., Urai, J.L., 2006. Fracture sealing and fluid overpressure in limestones of the Jabal Akhdar dome, Oman mountains. Geofluids 6, 168–184, http://dx.doi.org/10.1111/j.1468-8123.2006.00141.x.

Holland, M., Urai, J.L., Muchez, P., Willemse, E.J.M., 2009a. Evolution of fractures in a highly dynamic thermal, hydraulic, and mechanical system–(I) Field observations in Mesozoic carbonates, Jabal Shams, Oman Mountains. GeoArabia 14, 57–110.

Holland, M., Saxena, N., Urai, J.L., 2009b. Evolution of fractures in a highly dynamic thermal, hydraulic, and mechanical system–(II) Remote sensing fracture analysis, Jabal Shams, Oman Mountains. GeoArabia 14, 163–194.

Kulatilake, P.H.S.W., Wu, T.H., 1984. The density of discontinuity traces in sampling windows (technical note). International Journal of Rock Mechanics and Mining Sciences and Geomechanical Abstracts 21, 345–347.

Lacazette, A., 1991. A new stereographic technique for the reduction of scanline survey data of geologic features. Computers and Geosciences 17, 445–463, http://dx.doi.org/10.1016/0098-3004(91)90051-E.

LaPointe, P.R., 2002. Derivation of parent population statistics from trace length measurements of fractal populations. International Journal of Rock Mechanics and Mining Sciences 39, 381–388, http://dx.doi.org/10.1016/S1365-1609(02)00021-7.

Lee, C-H., Farmer, I., 1993. Fluid Flow in Discontinuous Rocks. Chapman & Hall, London, UK p. 169.

Loague, K., Green, R.E., 1991. Statistical and graphical methods for evaluating solute transport models: overview and application. Journal of Contaminant Hydrology 7, 51–73, http://dx.doi.org/10.1016/0169-7722(91)90038-3.

Lyman, G.J., 2003. Rock fracture mean trace length estimation and confidence interval calculation using maximum likelihood methods. International Journal of Rock Mechanics and Mining Sciences 40, 825–832, http://dx.doi.org/10.1016/S1365-1609(03)00043-1.

Manzocchi, T., Walsh, J.J., Bailey, W.R., 2009. Population scaling bias in map samples of power-law fault samples. Journal of Structural Geology 31, 1612–1626, http://dx.doi.org/10.1016/j.jsg.2009.06.004.

Markovaara-Koivisto, M., Laine, E., 2012. MATLAB script for analyzing and visualizing scanline data. Computers and Geosciences 40, 185–193, http://dx.doi.org/10.1016/j.cageo.2011.07.010.

Masoud, A.A., Koike, K., 2011. Auto-detection and integration of tectonically significant lineaments from SRTM DEM and remotely-sensed geophysical data. ISPRS Journal of Photogrammetry and Remote Sensing 66, 818–832, http://dx.doi.org/10.1016/j.isprsjprs.2011.08.003.

Mauldon, M., 1998. Estimating mean fracture trace length and density from observations in convex windows. Rock Mechanics and Rock Engineering 31, 201–216, http://dx.doi.org/10.1007/s006030050021.

Mauldon, M., Dunne, W.M., Rohrbaugh Jr., M.B., 2001. Circular scanlines and circular windows: new tools for characterizing the geometry of fracture traces. Journal of Structural Geology 23, 247–258, http://dx.doi.org/10.1016/S0191-8141(00)00094-8.

Neuman, S.P., 2005. Trends, prospects and challenges in quantifying flow and transport through fractured rocks. Hydrogeology Journal 13, 124–147, http://dx.doi.org/10.1007/sl0040-004-0397-2.

Odling, N.E., Gillespie, P., Bourgine, B., Castaing, C., Chilés, J.-P., Christensen, N.P., Fillion, E., Genter, A., Olsen, C., Thrane, L., Trice, R., Aarseth, E., Walsh, J.J., Watterson, J., 1999. Variations in fracture system geometry and their implications for fluid flow in fractured hydrocarbon reservoirs. Petroleum Geoscience 5, 373–384, http://dx.doi.org/10.1144/petgeo.5.4.373.

Pahl, P.J., 1981. Estimating the mean length of discontinuity traces. International Journal of Rock Mechanics and Mining Sciences & Geomechanics Abstracts 18, 221–228, http://dx.doi.org/10.1016/0148-9062(81)90976-1.

Pérez-Claros, J.A., Palmqvist, P., Olóriz, F., 2002. First and second orders of suture complexity in ammonites: a new methodological approach using fractal analysis. Mathematical Geology 34, 323–343, http://dx.doi.org/10.1023/A:1014847007351.

Pickering, G., Bull, J.M., Sanderson, D.J., 1995. Sampling power-law distributions. Tectonophysics 248, 1–20, http://dx.doi.org/10.1016/0040-1951(95)00030-Q.

Priest, S.D., Hudson, J.A., 1981. Estimation of discontinuity spacing and trace length using scanline surveys. International Journal of Rock Mechanics and Mining Sciences & Geomechanics Abstracts 18, 183–197, http://dx.doi.org/10.1016/0148-9062(81)90973-6.

Priest, S.D., 1993. Discontinuity Analysis for Rock Engineering. Chapman & Hall, London, UK p. 473.

Priest, S.D., 2004. Determination of discontinuity size distributions from scanline data. Rock Mechanics and Rock Engineering 37, 347–368, http://dx.doi.org/10.1007/s00603-004-0035-2.

Riley, M.S., 2005. Fracture trace length and number distributions from fracture mapping. Journal of Geophysical Research, 110, http://dx.doi.org/10.1029/2004JB003164.

Rohrbaugh Jr., M.B., Dunne, W.M., Mauldon, M., 2002. Estimating fracture trace intensity, density and mean length using circular scanlines and windows. AAPG Bulletin 86, 2089–2104, http://dx.doi.org/10.1306/61EEDE0E-173E-11D7-8645000102C1865D.

Roy, A., Perfect, E., Dunne, W.M., Mckay, L.D., 2007. Fractal characterization of fracture networks: an improved box-counting technique. Journal of Geophysical Research 112, B12201, http://dx.doi.org/10.1029/2006JB004582.

Spillmann, T., Maurer, H., Willenberg, H., Evans, K.F., Heincke, B., Green, A.G., 2007. Characterization of unstable rock mass based on borehole logs and diverse borehole radar data. Journal of Applied Geophysics 61, 16–38, http://dx.doi.org/10.1016/j.jappgeo.2006.04.006.

Terzaghi, R.D., 1965. Sources of error in joint surveys. Géotechnique 13, 287–304, http://dx.doi.org/10.1680/geot.1965.15.3.287.

Weiss, M., 2008. Techniques for estimating fracture size: a comparison of methods. International Journal of Rock Mechanics and Mining Sciences 45, 460–466, http://dx.doi.org/10.1016/j.ijrmms.2007.07.010.

Wilson, C.E., Aydin, A., Karimi-Farad, M., Durlofsky, L.J., Sagy, A., Brodsky, E.E., Kreylos, O., Kellog, L.H., 2011. From outcrop to flow simulation: constructing discrete fracture models from a LIDAR survey. AAPG Bulletin 95, 1883–1905, http://dx.doi.org/10.1306/03241108148.

Xu, C., Dowd, P., 2010. A new computer code for discrete fracture network modelling. Computers & Geosciences 36, 292–301, http://dx.doi.org/10.1016/j.cageo.2009.05.012.

Zeeb, C., Göckus, D., Bons, P.D., AlAjmi, H., Rausch, R., Blum, P., 2010. Fracture flow modelling based on satellite images of the Wajid sandstone, Saudi Arabia. Hydrogeology Journal 18, 1699–1712, http://dx.doi.org/10.1007/s10040-010-0609-x.

Zeeb, C., Gomez-Rivas, E., Bons, P.D., Blum, P. Evaluation of sampling methods for fracture network characterization using outcrops. AAPG Bulletin, http://dx.doi.org/10.1306/02131312042, in press.